DOI: 10.2478/jlecol-2026-0030 Journal of Landscape Ecology (2026), Vol: 19 / No. 3

SPATIOTEMPORAL EVALUATION OF LAND USE LAND COVER CHANGE IN JEMMA SUB-BASIN, UPPER BLUE NILE BASIN, ETHIOPIA

ABIRHAM CHERINET[1,2*], BELAY SIMANE[3], ABRAHAM MEBRAT ASMARE[1], HENOK ABATE DEMESSIA[1] AND YILKAL GEBEYEHU MEKONNEN[4,5]

[1]Institute of Disaster Risk Management and Food Security Studies, Bahir Dar University, P.O. Box 79, Bahir Dar, Ethiopia, E-mail: abrahammebrat@gmail.com
[2]Ethiopian Forestry Development, P.O. Box 33042, Addis Ababa, Ethiopia
[3]College of Development Studies, Addis Ababa University, P.O. Box 1176, Addis Ababa, Ethiopia, E-mail: simaneb@yahoo.com
[4]Department of Natural Resources Management, Debre Markos University, P.O. Box 269, Debre Markos, Ethiopia
[5]Department of Hydrology, University of Zululand, Kwa-Dlangezwa, Richards Bay 3886, Durban, South Africa, e-mail: yilkalg3@gmail.com
**Corresponding author email: aberham2010@gmail.com*

Received: 21st August 2025, **Accepted:** 18th March 2026

ABSTRACT

Land use land cover change (LULCC) is a complex phenomenon influenced by human activities and environmental factors that significantly affect ecosystems and sustainable development. To effectively understand this dynamic process and integrate it into planning and natural resource management, current and projected LULC information is crucial. This study aimed to assess the LULCC from 2003 to 2024 and project for the next 20 years in the Jemma sub-basin of Ethiopia. We employed random forest (RF) machine-learning algorithms for classification, and a CA-ANN model to project future LULC changes using the MOLUSCE plugin in QGIS. Elevation, distance from rivers, and distance from roads were used as inputs in the projection process. The major land use types identified in the study area were cropland, grazing land, water bodies, forest land, bare land, and built-up areas. Classification accuracy ranged from 83 % to 90 %, and the kappa coefficient ranged from 0.78 to 0.88. Between 2003 and 2024, cropland, built-up areas, and water bodies increased by 6.5, 2.3, and 0.2 %, respectively, while forest land increased by 1.7 %. Conversely, grazing and bare land decreased by 9.9 % and 0.7 %, respectively, between 2003 and 2024. In 2034, cropland, water bodies, forest land, and built-up areas are projected to increase by 1.99 %, 0.01 %, 0.56 %, and 0.18 %, respectively; however, these land use types show a slight decreasing trend from 2034 to 2044, except for built-up areas. Urban areas are expected to increase by 0.48 % between 2034 and 2044, primarily at the expense of grazing and bare lands. The findings suggest that significant land use changes are shaping the ecological and socioeconomic dynamics of the sub-basin. Therefore, promoting the wise utilization of natural resources and effective land management practices is essential to ensure ecological and environmental sustainability in the sub-basin.

Keywords: Artificial neural network; Google Earth Engine; machine learning algorithm; MOLUSCE plugin; QGIS; random forest

INTRODUCTION

Land use land cover change (LULCC) is a global phenomenon shaped by human activities and environmental factors (Gedefaw, 2023; Dastour *et al*., 2022; Afzal *et al*., 2021; Li *et al*., 2021; Oloukoi, 2018). Recent estimation shows that approximately 17 % of the planet's land has changed at least once between major land cover classes in recent decades (Winkler *et al*., 2021). The global cost of land degradation as a result of poor land management practices on crop and grazing land is estimated to be over 300 billion USD per year, with sub-Saharan Africa accounting for the largest share (22 %) of the global cost (Braun, 2016). Besides, the health and livelihoods of more than 1.5 billion people worldwide are significantly affected by land degradation, where women and disadvantaged groups are more vulnerable to its effects (Rehman *et al*., 2022; Tadese *et al*., 2021; Wakjira *et al*., 2020).

Ethiopia is among the Sub-Saharan countries where LULCC is intensively undergoing as a result of agricultural expansion, encroachment, urbanization, and deforestation (Moisa *et al*., 2022; Regasa *et al*., 2021; Dagnachew *et al*., 2020; Tolessa *et al*., 2017). Previous studies highlighted that significant LULCC has been observed in different parts of the country since the late twentieth century (Hishe *et al*., 2020; Minta *et al*., 2018; Feyissa & Gebremariam, 2018; Gebrehiwot *et al*., 2014). Studies focused on the Ethiopian highlands have highlighted that the expansion of cultivated land has occurred at the expense of natural forests over time (Betru *et al*., 2019; Minta *et al*., 2018; Gashaw *et al*., 2017). Therefore, accurate and effective monitoring of LULCC is imperative to develop policies to protect the environment and promote sustainable development (Zhao *et al*., 2023).

Currently, mapping land use and land cover, with various features on the earth's surface become easier due to advancements in remote sensing and GIS technology (Pande *et al*., 2024). Traditional geospatial methods require substantial data for classification when mapping high-resolution land cover across large areas. As a result, enormous storage capabilities, powerful processing, and the ability to use a variety of techniques are all necessary (Xie *et al*., 2019). Google Earth Engine (GEE) is a cloud-based platform that offers fundamental functionalities for the complex calculation of geospatial studies on a global scale (Amani *et al*., 2020; Gorelick *et al*., 2017), enhances the ability to process and analyze extensive satellite data efficiently, and provides time series data on land cover and usage (Pande *et al*., 2024).

Despite its difficulty due to stochastic changes in nature and socioeconomic variables (Wang & Zhang, 2014), LULC prediction is important to simulate future landscape conditions to understand their spatiotemporal trends and implement necessary measures in advance (Regasa *et al*., 2021). It is critical to predict future LULCC in areas where agriculture is a predominant source of income and the backbone of the country's economy (Dagnachew *et al*., 2020; Dibaba *et al*., 2020). Attempts have been made to predict future LULCC using different classification models, such as Artificial Neural Networks (ANNs) (Eshetie *et al.*, 2023), Cellular Automata (CA) (Al *et al*., 2021), CA-Markov Chain (CA-MC) (Gasirabo et al., 2023), CA-ANN (Baig et al., 2022). However, models have their strengths and weaknesses, which affect the prediction accuracy (Tessema *et al.*, 2020). This study applied CA-ANN algorithms to simulate future LULC of the study area. CA-ANN can precisely represent complex geographically heterogeneous areas and has been widely applied in LULCC analysis and prediction studies (Ateka *et al*., 2022; Girma *et al*., 2021; Mekonnen *et al*., 2018; Gashaw *et al*., 2017; Rahman *et al*., 2017).

Jemma sub-basin is one of the best grain producers and a leading supplier of sorghum in Ethiopia, and among the eight good-performing zones in crop production (Mare *et al*., 2024; Temeche *et al*., 2021). This sub-basin also contributes about 9 % of the annual flow and covers about 8 % of the total area of the Upper Blue Nile basin (ABDO, 2020). However, due to high population growth (CSA, 2007) and land-intensive development activities, various biophysical and socioeconomic problems have been a challenge in the study area and the country at large. In addition, the sub-basin has the most severe soil erosion rates in the entire Upper Blue Nile basin, due to poor land management (Betrie *et al*., 2011). Therefore, LULCC in the Jemma sub-basin and the prediction of future LULCC are vital to understanding the dynamics of human-environment interactions and environmental management interventions.

Some attempts have been made to assess the impacts of LULCC on streamflow, reservoir sedimentation, and land degradation at the watershed level across the Jema sub-basin (Woldekiros, 2023; Abrham Atile, 2021; Temam, 2018; Temam, 2018). However, this fragmented display of results may not show the reality of the sub-basin and goal-oriented decision-making processes. Therefore, understanding the LULCC and future scenarios of the sub-basin will contribute to the knowledge of land dynamics in the Nile basin and the Earth widely. Thus, the main objective of this study is to assess and predict the spatiotemporal changes of LULC using the Random Forest (RF) and CA-ANN algorithms across the sub-basin.

MATERIALS AND METHODS

Study Area Description

The study area is located in the Central Highlands of Ethiopia. Geographically, the sub-basin lies between 9° 0' 0" and 11° 0' 0" North and 38° 30' 0" and 41° 0' 0" East. The total area coverage of the sub-basin is approximately 15,803 km^2 (Fig. 1). The Jemma sub-basin drains from the North Shewa zones of the Amhara and Oromia regions. The annual rainfall and temperature of the sub-basin range from 697 to 1475 mm and from 9 to 24°C, respectively. Whereas, the elevation of the sub-basin ranges from 1040 m to 3814 m above sea level. Crop cultivation and livestock rearing are the major livelihoods of the inhabitants. Based on the FAO's soil classification, the sub-basin is characterized by a diverse range of soil types, including Eutric Vertisols (28.07 %), Lithic Leptosols (37.44 %), Chromic Lixisols (8.07 %), Pelvic Vertisols (6.82 %), Haplic Luvisols (5.79 %), and Haplic Acrisols (6.82 %). However, the soil type found in a smaller portion in the lower part of the sub-basin is Eutric Fluvisols, Umbria Nitisols, and Alic Nitisols. The major soil texture observed in the sub-basin is sandy and clay loam (Ali *et al.*, 2015; Worku *et al*., 2021).

Fig. 1: Map of the study area.

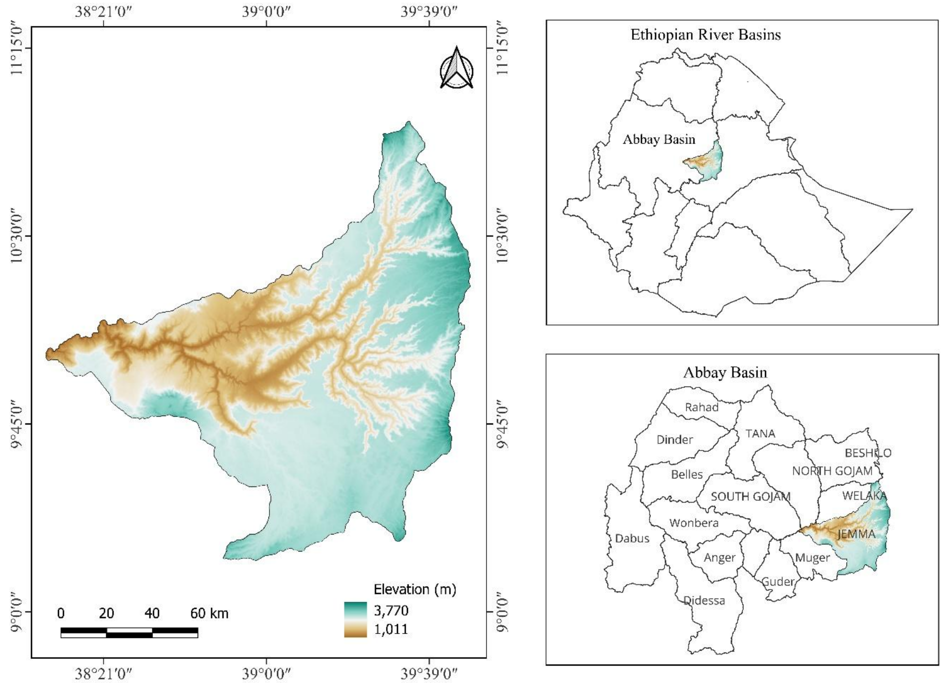

Data and Sources

Satellite Data

This study used the Shuttle Radar Topography Mission (SRTM) digital elevation model (DEM) and Landsat time series images, accessed from the USGS non-commercial image data source through the Google Earth Engine (GEE) Catalog (Table 1). The slope of the sub-basin was calculated using the SRTM DEM with a 30 m x 30 m spatial resolution. The 2003 satellite image was obtained from Landsat 7 ETM before the Scan Line Corrector was turned off, with less than 5 % cloud cover, while Landsat 8 OLI was used for 2014 and 2024. To obtain cloud-free images and minimize major variations in vegetation phenology and primary productivity, we collected images during the dry season (January-April).

Table 1: Landsat image data used for the analysis of land use and land cover (LULC).

Data	Used bands	Spatial resolution	Year
Landsat 7 ETM+	1–5, and 7	30m	2003
Landsat 8 OLI	2–7	30m	2014 and 2024
SRTM DEM	-	30 m	

Developing Training and Validation Samples

Machine learning algorithms for land-use classification rely on well-defined training points (Kasahun & Legesse, 2024). To obtain empirical data for LULC classification and accuracy evaluation, we interviewed local elders about well-known landmarks in the area, which served as the basis for collecting reference data for 2003. Consequently, training and validation samples were collected manually through visual interpretation of high-resolution Google Earth images (Sousa *et al*., 2020). Accordingly, 1100, 1178, and 1200 representative sample points were collected from each LULC class for 2003, 2014, and 2024, respectively. For larger LULC classes, more training points were collected (Fig. 2).

Fig. 2: Training points collected for the year 2003(a), 2014(b), and 2024(c).

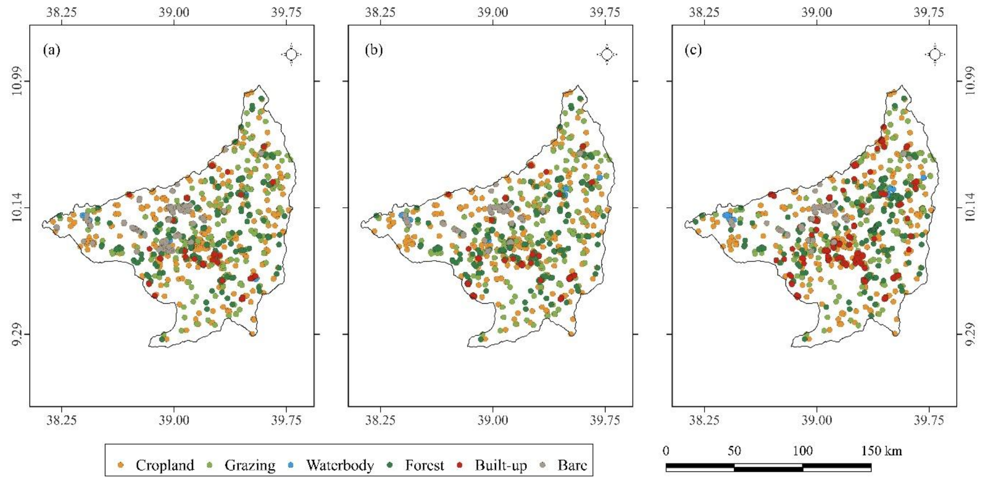

LULC Classification

Image classification was performed using a random forest classifier algorithm within the GEE platform. We used this classifier because it is a powerful and widely used algorithm for LULC classification (Amani *et al*., 2019; Kelley, 2018; Millard & Richardson, 2015). Moreover, this algorithm handles outliers and noisier datasets. Compared with other classifiers, it achieves higher accuracy and processing speed by selecting important variables (Mahdianpari *et al*., 2017; Beijma *et al*., 2014). Different vegetation indices, including the Normalized Difference Vegetation Index (NDVI), Soil Adjusted Vegetation Index (SAVI), Bare Soil index (BSI), Normalized Difference Water Index (NDWI), Modified Normalized Difference Water Index (MNDWI), Normalized Difference Built-up index (NDBI), and Principal Components (PCs) were used to improve the classification accuracy. These indices were computed as follows

$$NDVI = \frac{(NIR - RED)}{(NIR + RED)}$$

Where NIR is the Near Infrared band (Band 4 for Landsat 7 and Band 5 for Landsat 8), and RED is the red band.

$$SAVI = \frac{(NIR - RED)}{(NIR + RED + L)}$$

Where L is a soil brightness correction factor. L value 0.5 was used.

$$BSI = \frac{(SWIR1\ -\ RED)}{(SWIR1 +\ RED)}$$

SWIR1 is band 5 of Landsat 7 and band 6 of Landsat 8.

$$NDWI = \frac{(Green\ -\ NIR)}{(Green +\ NIR)}$$

Green is band 2 for Landsat 7 and band 3 for Landsat 8

$$MNDWI = \frac{(Green\ -\ SWIR1)}{(Green +\ SWIR1)}$$

$$NDBI = \frac{(SWIR1\ -\ NIR)}{(SWIR1\ +\ NIR)}$$

Accuracy Assessment

Accuracy assessment is conducted using reference pixels to create an error matrix that shows how well the ground truth is represented and verifies how closely the classified map matches the actual land cover (Abbas & Jaber, 2020; Shao *et al*., 2019; Haque, 2016). The study used 25 % of the collected sample points for accuracy assessment and the remaining 75 % for classification. The classification accuracy was determined using a confusion matrix, including user's accuracy (UA), the producer's accuracy (PA), the overall accuracy (OA), and the kappa coefficient (Sarkar, 2019).

$$Overall\ accuracy = \frac{Total\ number\ of\ correctly\ classified\ pixels(Diagonal)}{Total\ number\ of\ reference\ pixels} \times 1OO$$

$$Users\ Accuracy = \frac{\text{Samples correctly idntified in the raw}}{\text{Raw total}} \times 100$$

$$Producer\ Accuracy = \frac{Samples\ correctly\ identified\ in\ the\ column}{Column\ total} \times 100$$

$Kappa\ coefficient$

$$KC = \frac{(Total\ sample \times corrected\ sample) - \sum(Columen\ total \times Row\ total)}{Total\ sample^2 - \sum(Columen\ total - Row\ total)} \times 100$$

LULC Change Trend Analysis

LULC trend analysis was conducted to understand which land cover class is shifting to another land cover class (Tewabe & Fentahun, 2020). Thus, trend analysis for the Jemma sub-basin was conducted for the period between 2003 and 2014, and 2014 and 2024. Each LULC class in the sub-basin was compared, and the direction of shift was determined within the selected study time. The magnitude of the changes between the two periods was used to quantify the percentage and rate of change, which was computed as follows.

$$Rate\ of\ change\left(\frac{km^2}{year}\right) = \frac{A2 - A1}{Z}$$

where A2 is the LULC (km^2) area in period 2, A1 is the LULC (km^2) area in period 1, and Z is the period interval in years between A2 and A1.

Loss = Row total – diagonals of each class
Gain = column total – diagonals of each class
Net change = gain – loss
Net persistence change/diagonals of each class

Land Use Land Cover Change Prediction

A module for land use change simulation and evaluation (MOLUSCE) within the QGIS plugin was employed to assess future LULC conditions and spatiotemporal transitions. The plugin is preferable for the analysis of land use and forest cover change across various time frames (Albut, 2024). Cellular Automata-Artificial Neural Network (CA-ANN) machine learning algorithms were used to project the future LULCC. CA-ANN algorithms can provide more practical outcomes for LULC change analysis (Rehman *et al*., 2022; Kafy *et al*., 2021; Tolentino *et al*., 2021). The ANN parameters include a neighborhood of 1 pixel, a learning rate of 0.01, a maximum number of iterations of 1000, a hidden layer of 12, and a momentum of 0.05.

The model used 5,000 randomly sampled data points to provide a spatial representation for the ANN. To generate prediction maps, we used classified maps from 2003, 2014, and 2024 as the input dataset. The projection of LULC was performed for the next 20 years, extending from 2025 to 2044. Elevation, distance from roads, and distance from water bodies were considered as additional raster layers in the MOLUSCE to improve simulation accuracy. These spatial variables affected urban expansion over the last three decades, which had a significant influence on the predicted results of LULC. The distance maps were created in the ArcGIS Euclidean Distance tool. During the simulation process we integrate these dependent variable maps with the initial (2014) and final (2024) LULC maps. According to Gashaw *et al*. (2017), the slope was believed to be a similar limitation for the cultivated land and built-up area categories because both remain inhabited as the slope increases. The LULC category for forest and shrubland, on the other hand, did not consider slope to be a constraint. The methodological flowchart for both the detection and prediction is shown in Fig. 3.

Fig. 3: Methodological flowchart.

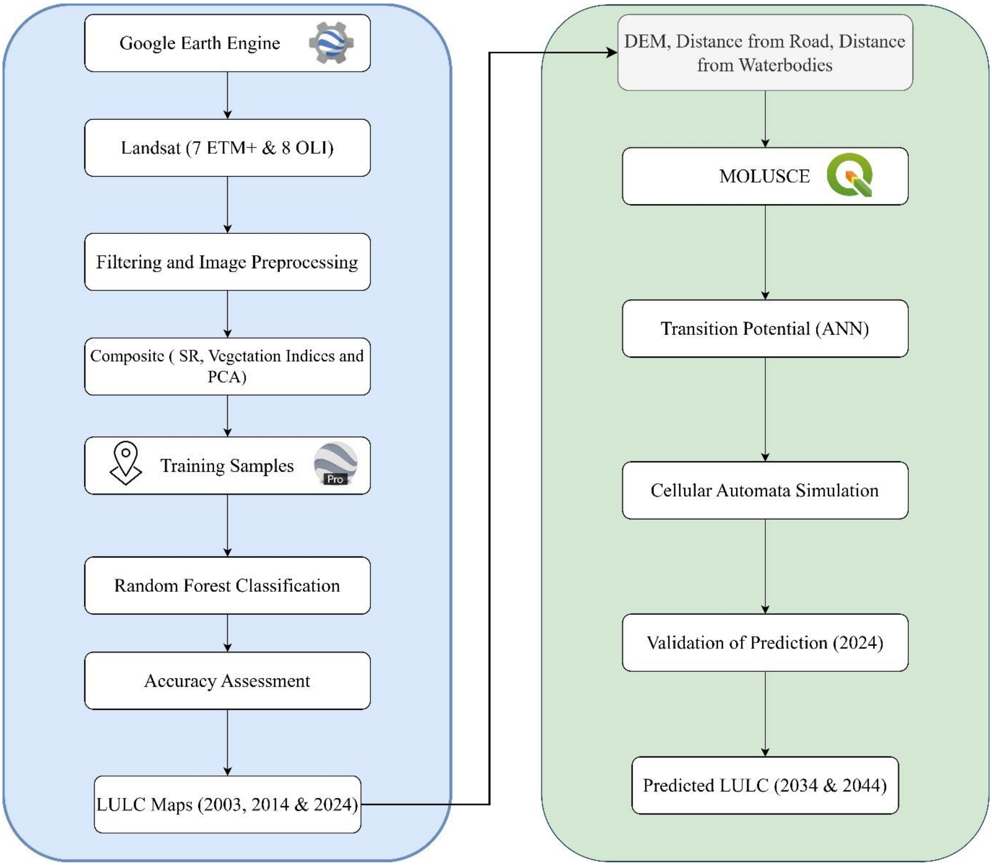

RESULTS AND DISCUSSIONS

Accuracy Assessment

Accuracy assessment was conducted for the classified maps of 2003, 2014, and 2024 to evaluate the agreement between the produced maps and the actual ground conditions. The overall results of the accuracy assessment ranged from 83 % to 90 %, while the Kappa coefficient was between 0.78 and 0.88 (Table 2). It revealed that all classified LULC maps achieved relatively high accuracy for further LULC change analyses (Alawamy *et al*., 2020). However, the accuracy of water bodies fluctuated, with the highest user accuracy observed in both 2014 and 2024. Similarly, the accuracy assessment for built-up areas varied significantly across the years.

Table 2: Accuracy assessment results for the years 2003, 2014, and 2024.

LULC classes	2003		2014		2024	
	Producer	User	Producer	User	Producer	User
Cropland	0.81	0.85	0.94	0.85	0.91	0.90
Grazing	0.81	0.70	0.80	0.86	0.83	0.83
Waterbody	1.00	0.83	1.00	0.92	0.80	1.00
Forest	0.86	0.88	0.85	0.91	0.97	0.89
Built up	0.73	0.80	0.88	0.91	0.94	0.94
Bare land	0.85	0.97	0.83	0.88	0.79	1.00
Overall	0.83		0.88		0.90	
Kappa	0.78		0.84		0.88	

LULC Classification of Jemma Sub-Basin (2003-2024)

The identified LULC types in the study area include cropland, grazing, water bodies, forest land, built-up areas, and bare land (Fig. 4). Each land use type and change is discussed in detail below.

Cropland

Cropland is the dominant land use type in the Jemma sub-basin, followed by grazing and forest lands. The area coverage of cultivated land in 2003, 2014, and 2024 was 769,552.04, 813,977.46, and 871,435.79 hectares, respectively (Table 3). This indicates that cropland has increased by 2.8 % from 2003 to 2014 and by 6.5 % from 2003 to 2024. In general, cropland has increased by 101,883.75 ha, with an average annual rate of 4,631.08 ha between 2003 and 2024 (Table 4).

Table 3: Land use land cover dynamics of Jemma sub-basin over the past 20 years (2003–2024).

Land cover	2003		2014		2024	
	Area (ha)	%	Area (ha)	%	Area (ha)	%
Cropland	769552.04	48.7	813977.46	51.5	871435.79	55.2
Grazing	628403.95	39.8	566412.09	35.9	472865.23	29.9
Waterbody	1898	0.1	2576.5	0.2	4180.46	0.3
Forest	134479.96	8.5	151209	9.6	161293.02	10.2
Built up	11557.05	0.7	17521.32	1.1	47991	3.0
Bare land	33448	2.1	27642.63	1.8	21573.5	1.4
Total	1579339	100	1579339	100	1579339	100

Grazing Land

The grazing land in the sub-basin showed a declining trend (Table 3). This land use type in the Jemma sub-basin decreased by 3.9 % (2003-2014), 6 % (2014-2024), and 9.9 %

(2003-2024). A total of 155,538.7 ha of grazing land converted to other land use types between 2003 and 2024, with an annual declining rate of 7,069.9 ha (Table 4). This finding underscores that the grazing land was dominantly converted to cultivated land and settlement.

Water Body

Water bodies in the sub-basin showed an increasing trend (Table 3). It covers 0.1 % (1,898 ha), 0.2 % (2,576.5 ha), and 0.3 % (4,180.46 ha) of the total area of the sub-basin in 2003, 2014, and 2024, respectively. The annual rate of increment in the water body was 61.7 ha in 2003 and 2014, and 145.8 ha between 2014 and 2024. This finding suggests that the increase in water bodies in the sub-basin may be due to the construction of small-scale irrigation schemes, enhanced water management practices, and conservation measures.

Table 4: Rate of change from 2003 to 2024.

Land cover	2003-2014	2014-2024	2003-2024	Annual Rate of Change (ha)		
				2003-2014	2014-2024	2003-2024
Cropland	44425.42	57458.33	101883.75	4038.67	5223.48	4631.08
Grazing	-61991.86	-93546.86	-155538.72	-5635.62	-8504.26	-7069.94
Waterbody	678.50	1603.96	2282.46	61.68	145.81	103.75
Forest	16729.04	10084.02	26813.06	1520.82	916.73	1218.78
Built up	5964.27	30469.68	36433.95	542.21	2769.97	1656.09
Bare land	-5805.37	-6069.13	-11874.50	-527.76	-551.74	-539.75

Forest Land

Forest land coverage of the Jemma sub-basin was 8.5 % (134,479.96 ha), 9.6 % (151,209 ha), 10.2 % (161,293.02 ha), and 9.69 % (153,080 ha) in 2003, 2014, and 2024, respectively. The result shows that forest land has increased slightly since 2003. According to FGD participants, the widespread planting of eucalyptus trees and area closures are the major reasons for the increase in forest cover in the study area. Research findings show that plantation land has increased in different parts of the country.

Built up

Ethiopia, in general, and the Jemma sub-basin in particular, are experiencing significant urban expansion over recent decades, leading to a substantial increase in built-up areas. Built-up areas in the study area were 0.7 % (11,557.05 ha) in 2003, 1.1 % (17,521.32 ha) in 2014, and 3.0 % (54,030 ha). Regarding the rate of change, built-up area increased by 542.2 ha per year between 2003 and 2014 and by 2,770 ha between 2014 and 2024. According to the local community and focus group discussants, the need for shelter, construction of industries, and factories are the primary reasons for the increase in settlement area in the study area.

Bare Land

Bare land is an area of land that has little to no vegetation cover and is largely devoid of human structures or significant land use. The bare land of the study area shows a continuous decline over the study period. Out of the total area of the sub-basin in 2003, bare land constituted about 2.1 % (33,448 ha). However, the total bare land coverage of the Jemma sub-basin was 1.8 % (27,642.63 ha) and 1.4 % (21,573.5 ha) in 2014 and 2024 (Table 3). This decline in the bare land was attributed to the widespread implementation of plantations (afforestation and reforestation), soil and water conservation activities, and area closure efforts.

Fig. 4: LULC map for 2003, 2014, and 2024.

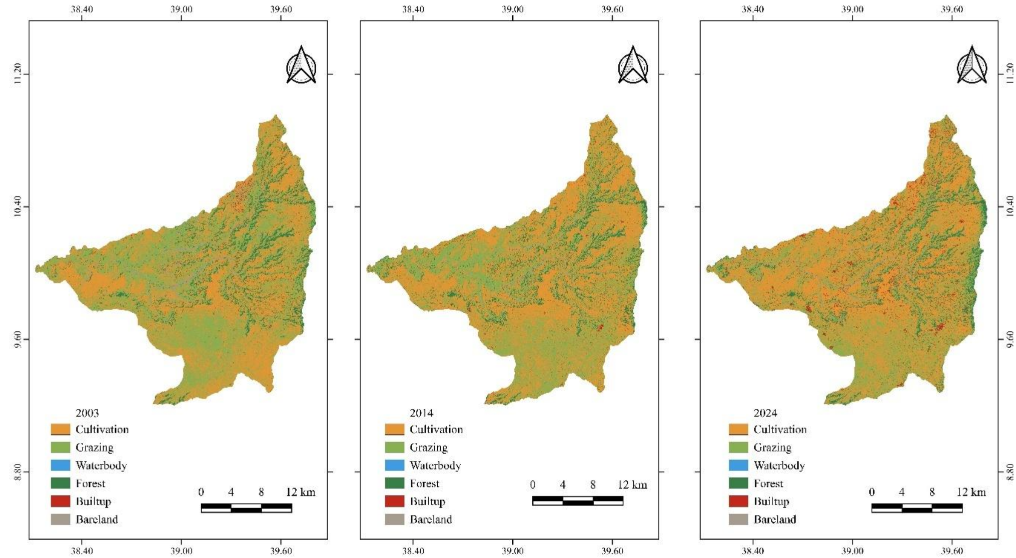

Transition Probability Matrix (TPM)

The probability of LULCC conversion from one land use type to another was summarized in Tables 5 and 6. The diagonal, which is bolded, depicted the remaining land use types, whereas the other values indicated the likelihood of changing land use type from one land use type to another in the sub-basin. About 590,514.89 ha of cropland remained unchanged between 2003 and 2014. The major contributors to crop lands were grazing, forest, and bare land. Grazing land contributed about 197,795.14 ha for cropland, and 11.1 % (8,413.11 ha) of forest land was converted to cropland between 2003 and 2014. Similarly, about 14,738.57 ha (1.9 %), 4,811.79 ha (0.4 %), and 5,564.52 ha (0.6 %) of the cropland were converted to forest land, bare land, and built-up, respectively. The conversion of cropland to other lands could emanate from land abandonment and land degradation. The result shows no conversion of the LULC class from built-up to water body from 2003 to 2014. In addition, approximately 50,633 ha of grazing land were converted to forest land and built-up areas due to reforestation initiatives and urban encroachment into grazing lands. The result further revealed that a considerable portion of forest land was also converted to grazing land, 24.9 % (32,863.01 ha), between 2003 and 2014.

Table 5: Transition area matrix (ha) of LULC between 2003 and 2014.

	LULC class	2014							
		Cropland	Grazing	Waterbody	Forest	Built up	Bare land	Sum	Loss
2003	Cropland	**590514.89**	153645.20	277.07	14738.57	5564.52	4811.79	769552.04	173472.63
	Grazing	197795.14	**378576.99**	49.15	46408.46	4224.71	1349.50	628403.95	249826.96
	Waterbody	130.13	18.30	**1441.16**	43	7	258.41	1898	456.84
	Forest	8413.11	32863.01	144.04	**89764.79**	3148.50	146.51	134479.96	44715.17
	Built up	950.67	847.34	0	64.89	**9651.36**	42.79	11557.05	1905.69
	Bare land	10609	461.25	665.08	189.29	489.75	**21033.63**	33448	12414.37
Column sum		808412.94	566412.09	2576.5	151209	23085.84	27642.63	–	–
Gain		217898.05	187835.1	1135.34	61444.21	7869.96	6609	–	–
Net change		44425.42	-61991.86	678.5	16729.04	5964.27	-5805.37	–	–
Net persistent		0.075	-0.164	0.471	0.186	0.617	-0.276	–	–

Table 6: Transition area matrix (ha) of LULC between 2014 and 2024.

	LULC class	2024 Cropland	Grazing	Waterbody	Forest	Built up	Bare land	Sum	Loss
2014	Cropland	**675,953.01**	99,925.82	810.47	12,952.29	18,857.04	5,478.83	813,977.46	138,024.45
	Grazing	178,401.80	**332,945.36**	912.04	44,714.23	8,953.13	485.53	566,412.09	233,466.73
	Waterbody	205.05	51.43	**978.07**	580.42	17.88	743.65	2576.50	1598.43
	Forest	9,455.75	36,084.04	830.39	**102,379.29**	2,287.32	172.21	151,209.00	48,829.71
	Built up	2,544.17	3,514.96	17.26	233.75	**10,509.44**	701.74	17,521.32	7,011.88
	Bare land	4,876.01	343.62	632.23	433.04	7,366.19	**13,991.54**	27,642.63	13,651.09
Column sum		871,435.79	472,865.23	4,180.46	161,293.02	47,991.00	21,573.50	–	–
Gain		195,482.78	139,919.87	3,202.39	58,913.73	37,481.56	7,581.96	–	–
Net change		57,458.33	-93,546.86	1,603.96	10,084.02	30,469.68	-6,069.13	–	–
Net persistent		0.085	-0.281	1.640	0.098	2.899	-0.434	–	–

Furthermore, between 2014 and 2024, forest land, water bodies, and built-up areas increased significantly at the expense of crop land. The result further revealed that, about 178,401.80, 44,714.23, and 8,953.13 hectares of grazing land were converted to crop land, forest land, and built-up areas, respectively. The ongoing conversion of cropland and grazing land to settlement underscores the need for integrated land use planning and sustainable management practices. The increasing number of inhabitants in the sub-basin is the potential reason for the conversion of bare land to cropland and built-up areas to meet the growing demand for food and shelter. Despite the complexity of LULCC transition among urbanization, cropland expansion, degradation, and environmental conservation, there is a positive outcome in forest land expansion.

Net Gain/Loss Across Different Land Use Classes

The net gains and net losses of LULC between 2003–2014, and 2014–2024 are presented in Fig. 5. Regarding net gain and loss, cropland increased by about 44,425.42 hectares between 2003 and 2014 and by approximately 57,458.33 hectares from 2014 to 2024 across different land use classes. This upward trend may be due to increased agricultural production, possibly driven by food demand. Grazing land experienced significant losses in both decades, with 61,991.86 hectares lost between 2003 and 2014, and about 93,546.86 hectares of grazing land converted to other land use classes between 2014 and 2024. The rate of grazing land loss appears to have accelerated in the second period, likely due to ongoing cropland expansion. Water bodies have steadily increased over the past decades, with a notable rise of 1,603.96 hectares between 2014 and 2024, driven by reservoir construction and water conservation efforts to support agriculture and drinking water supply.

Forest land gained about 16,729.04 and 10,084.02 ha in the first and second periods, respectively. This could be due to widespread plantation initiatives such as the Reducing Emissions from Deforestation and Forest Degradation (REDD+) programme, and community-based physical and biological conservation practices. Specifically, improving farmers' interest in converting crop and grazing lands to eucalyptus plantations as a cash crop could be a possible reason for the expansion of forest land. Built-up areas show a modest increase (5,964.27 ha) between 2003 and 2014, whereas a significant increase (30,469.68 ha) was observed between 2014 and 2024. This indicates rapid urbanization, infrastructure expansion, and industrialization in response to population growth and economic expansion.

Bare land is one of the continuously declining land use classes throughout the study period. The highest loss (6,069.13 ha) of bare land was recorded from 2014 to 2024; the net loss of bare land cover over the entire study period was 11,874.5ha, with an annual rate of 539.8 hectares (Table 6). The reduction in bare land is attributed more to the conversion to more productive land uses, such as cropland and urban development. Area closure, afforestation, and reforestation activities are also possible factors to reduce bare land. In general, cropland, water bodies, and built-up areas show a consistent increase, while grazing land and bare land decreased significantly. This result underscores the dynamic interplay between urbanization, cropland expansion, environmental conservation, and changing land use practices that shaped the landscape over time.

Fig. 5: Gains and losses graph between 2003–2014, and 2014–2024 in hectares.

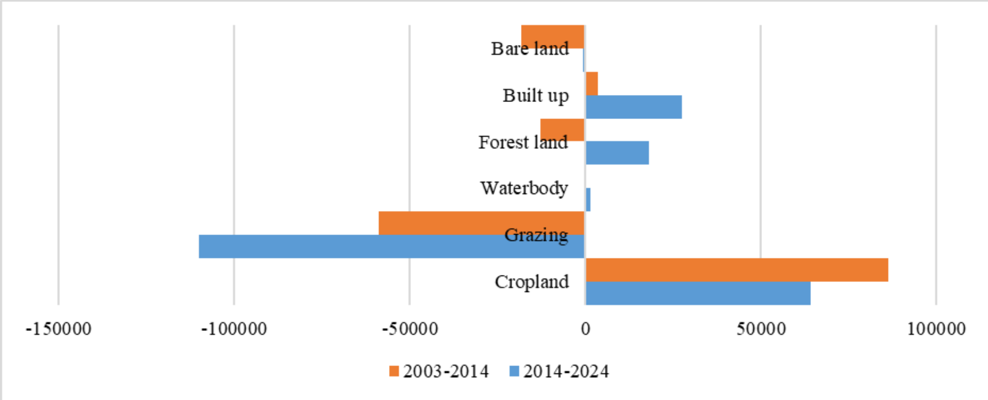

LULC Projection of Jemma Sub Basin

After selecting the relevant spatial variables, creating factor maps, and conducting geometry matching was computed (Fig. 6). Pearson's correlation result shows a strong correlation (0.99) between distance from the main road and distance from streams. In addition, elevation was also strongly correlated with distance from main roads (0.91) and distance from streams (0.89).

Fig. 6: Input layer nodes: distance from road, distance from river, and elevation.

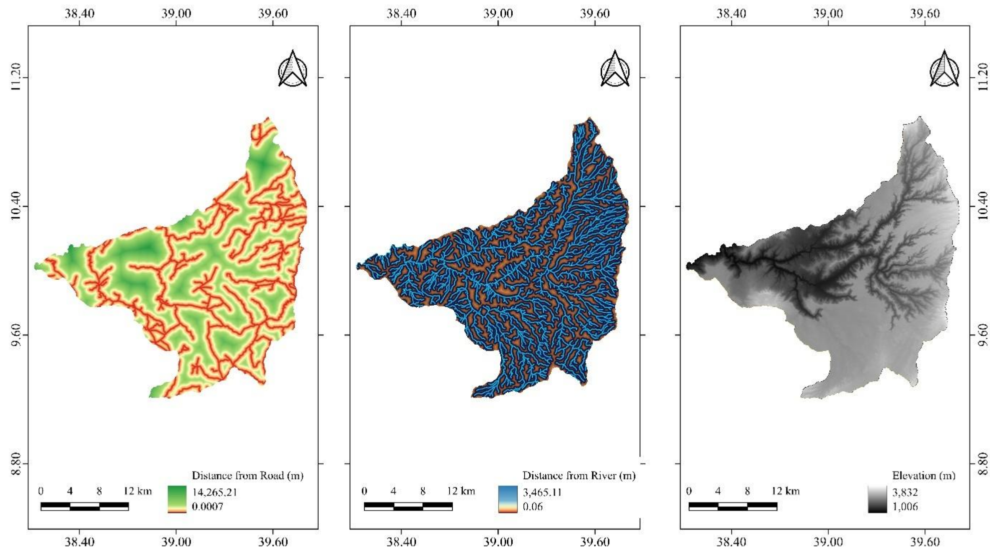

Actual and Simulated LULC of Jemma Sub-Basin for 2024

During the determination of the predicted LULC change, the CA-Markov model validation result indicated a high level of agreement between observed and projected 2024 LULC maps. The ANN simulation results in an overall accuracy of -0.0018, a minimum validation error of 0.031, and a validation kappa of 0.98. The validation statistics between the predicted 2024 and observed 2024 LULC maps indicated a correctness of 73 %, with a kappa (overall) of 0.53, a kappa (histogram) of 0.88, and a kappa (location) of 0.6. The overall result indicates a moderate level of agreement between the two map categories. Accordingly, the actual and simulated 2024 maps depicting cropland and grazing land areas show a slight increase of 1.46 % and 0.14 %, respectively. Whereas, water bodies, forest land, and bare lands slightly decrease within a range of -0.05 to 1.12 %. In general, the area coverage of the two periods showed that all land use land cover classes have the best range of agreement, with a rate of difference lower than 10 % (Table 7). Thus, the land use maps from 2014 to 2024 were used to anticipate 2034, and similarly, output maps of 2024 and 2034 were used to project the 2044 LULC.

Table 7: LULC change prediction validation based on the actual and projected 2024 LULC.

LULC class	Actual 2024		Simulated 2024		Changes	
	Area (Ha)	Area (%)	Area (Ha)	Area (%)	Rate of change	Percentage
Cropland	871435.79	55.2	894866.71	56.66	23430.92	1.46
Grazing	472865.23	29.9	474443.64	30.04	1578.41	0.14
Waterbody	4180.46	0.3	3903.50	0.25	-276.96	-0.05
Forest land	161293.02	10.2	143335.72	9.08	-17957.30	-1.12
Built up	47991.00	3.0	48323.69	3.06	332.69	0.06
Bare land	21573.50	1.4	14465.74	0.92	-7107.76	-0.48
Total	1579339	100	1579339	100		

LULC Change Simulation and Prediction Using the CA-ANN Model

The projected land use cover types for 2034 and 2044 were computed using the CA-Markov model, with the results presented in Table 9 and the area shown in Fig. 7. The simulation results indicate that cropland, water bodies, forest land, and built-up areas are likely to continue increasing in 2034 and 2044. In terms of percentage, cropland expands from 55.2 % in 2024 to 57.28 % in 2034, reflecting a 2 % increase. The persistent expansion of cropland continues from 2034 to 2044 at an average growth rate of 1.71 %. In other words, cropland increased by 33,273 ha and 26,916.3 ha between 2024 and 2034 and between 2034 and 2044, respectively. The persistent expansion of cropland is attributed to the need to meet food demand due to rapid population growth. Built-up areas have increased by 0.21 % (2,653 ha) from 2024 to 2034 and 0.48 % (7,675 ha) from 2034 to 2044. The ongoing urbanization and infrastructure development to meet the needs of the growing population and economic activities could be the potential reason. Water bodies in the study area are also projected to increase slightly on average, 0.26 % to 0.30 % between 2024 and 2044, indicating modest expansion of water features over the next two decades. This could be due to the widespread construction of small dams and reservoirs for irrigation and domestic uses. Ethiopia's irrigation development plan indicates that the government is actively pursuing a comprehensive strategy to enhance irrigation infrastructure, aiming to boost agricultural productivity, ensure food security, and promote economic growth. The projection suggests that forest land will increase by 0.1 % from 2024 to 2034 and by 0.12 % between 2034 and 2044. This growth can be attributed to the widespread implementation of mass plantation initiatives such as the Green Legacy Initiative (GLI), the Reducing Emissions from Deforestation and Forest Degradation (REDD+) program, and community-based conservation practices.

Grazing and bare land areas are projected to decrease significantly in both periods. For example, grazing land decreased from 29.94 % (472,865 ha) in 2024 to 28.02 % in 2034 and from 28.02 % in 2014 to 25.88 % in 2044, a reduction of 2.14 %. Conversion of grazing land to crop land, urban development, and changes in land management practices may be among the potential reasons for the decrease. Similarly, bare land decreased from 1.37 % (21,574 ha) in 2024 to 0.72 % in 2044.

Table 8: The area coverage, percent, and rate of change between 2024, 2034, and 2044.

LULC class	2024		2034		2044	
	Area (ha)	Area (%)	Area (ha)	Area (%)	Area (ha)	Area (%)
Cropland	871,436	55.18	904,709	57.28	931,625	58.99
Grazing	472,865	29.94	442,587	28.02	408,698	25.88
Waterbody	4180	0.26	4516	0.29	4712	0.30
Forest land	161,293	10.21	162,865	10.31	164,685	10.43
Built up	47,991	3.04	50,644	3.21	58,319	3.69
Bare land	21,574	1.37	14,018	0.89	11,300	0.72
Total	1,579,339	100	1,579,339	100	1,579,339	100

The projection revealed that the forest area increased slightly from 10.21 % (161,293 ha) in 2024 to 10.31 % (162,865 ha) in 2034 and to 10.43 % (164,685 ha) in 2044. This positive trend is potentially associated with the governments and the community's widespread participation in afforestation and reforestation activities. The overall LULCC trend in Fig. 8 shows that all land use classes have increased over the entire period, except for grazing and bare lands.

Fig. 7: Predicted 2034(a) and 2044(b) LULC of Jemma sub-basin.

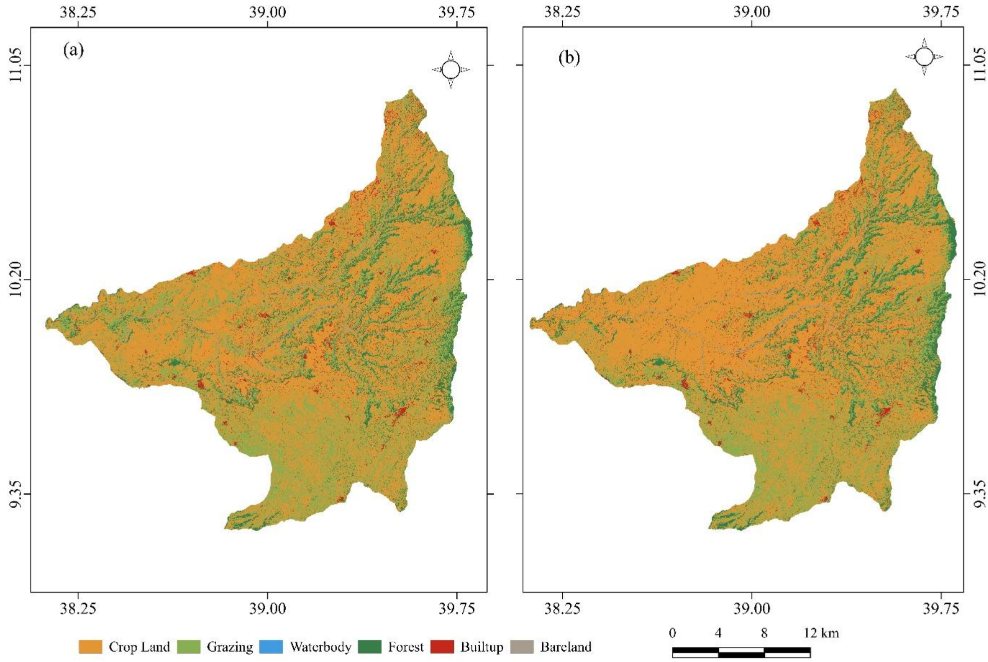

Fig. 8: Trends of land use/land cover changes from 2003 to 2044 in the Jemma sub-basin.

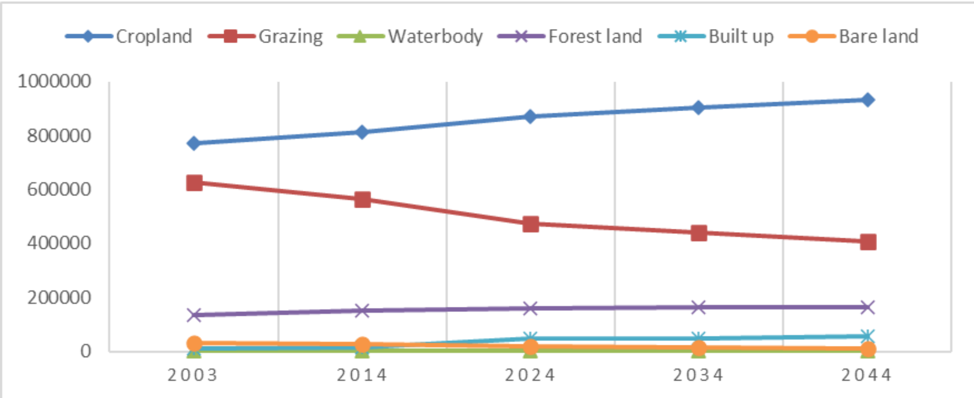

DISCUSSION

In this study, we examined past, present, and future LULC change dynamics in the Jemma sub-basin using an integrated approach. Assessing historical LULC and forecasting future trends are crucial for understanding current natural resource utilization and guiding sustainable land management. The overall classification accuracy ranged from 83 % to 90 %, and the kappa coefficient ranged from 0.78 to 0.88, which is within the acceptable range for further LULC change detection. The findings revealed that cropland increased by 2.8 % from 2003 to 2014 and by 3.7 % from 2014 to 2024. This significant expansion of cultivated land could be driven by escalating demand for food production. Cultivated land of the study area is still expanding to a greater extent at the expense of grazing and forest lands at different stages. This finding implied that the landscape is susceptible to anthropogenic actions. Similar findings also indicated the presence of significant expansion of cultivated land in various parts of Ethiopia (He & Chen, 2022; Kuma *et al*., 2022; Abebe *et al*., 2021; Hailu *et al*., 2020; Cherinet, 2019).

Built-up areas of the study area increased at a considerable annual rate of 542.2 ha between 2003 and 2014 and 2,770 ha from 2014 to 2024. According to the CSA 2007, the inhibitors of the Jemma sub-basin are increasing with an annual growth rate of 1.7. Therefore, the need for shelter, construction of industries, and factories are the primary reasons for the increase in settlement area in the study area. Different studies across the country revealed the presence of a significant increase in built-up area expansion because of population growth, infrastructure development, and policy initiatives (Agona & Abebe, 2024; Leta & Demissie, 2021; Halefom *et al*., 2018; Dibaba *et al*., 2020; Gashaw *et al*., 2017). Effective land-use management strategies should be implemented by policymakers and urban planners, including promoting efficient land use, reducing urban sprawl, and preserving green spaces, contributing to the attainment of Sustainable Development Goal (SDG) 11, which focuses on creating sustainable cities and communities.

The classification result shows that forest land increased slightly since 2003. According to FGD participants, the widespread planting of eucalyptus trees and area closures are the major reasons for the increase in forest cover in the study area. This result is further supported by the Ethiopian Forestry Development 2023 report, which states that Ethiopia's forest cover rose from 17.2 % in 2019 to 23.6 % in 2023 (EFD, 2024). Research findings show that plantation land has increased in different parts of the country. For example, a study by Amiga *et al*. (2024) found that the area of Eucalyptus plantations increased from 12 % in 2000 to 20 % in 2021. Another result reported by Molla & Addisie (2023) also indicated that the area of Eucalyptus plantations increased from 908.87 hectares in 1991 to 26,261.9 hectares in 2021. Similarly, Belay *et al*. (2023) and Negasa *et al* (2016) indicated that Eucalyptus plantation coverage increased significantly in the Meja watershed and the Senan district. This expansion is attributed to the expense of fertile cultivated land and grazing land. Land size, market accessibility, due to its low labor and capital requirements, and higher incomes, and lower production costs are the major factors that lead farmers to shift their interests toward eucalyptus plantations (Wasie, 2024; Belay *et al*., 2023).

Water bodies are the other land-use type in the sub-basin, slightly increasing over the study period. The finding suggested that the increase in water bodies in the sub-basin could be due to the construction of small-scale irrigation schemes, enhanced water management practices, and conservation measures. Various studies have documented an increasing number of water bodies across the country (Amsalu & Mekonen, 2024; Getaneh *et al*., 2024; Shibeshi & Venkatesham, 2024; Ayele *et al*., 2023).

Grazing and bare lands showed a continuous declining trend over the study period. The results further revealed that a total of 155,538.7 ha of grazing land and 49,216.13ha of bare land were converted to other land use types between 2003 and 2024. This finding underscores that the grazing land was dominantly converted to cultivated land and settlement. According to the focus group discussants, land degradation for cultivation, over grazing, encroachment of settlement construction, and drought are responsible factors for the persistent decline of grazing land. In line with our results, a study in the Gudo Beret watershed found that grazing land declined substantially, whereas cropland and plantation areas increased significantly (Mekuria *et al*., 2018). A similar finding was also reported by Kindu *et al*. (2013) and Ogato *et al*. (2021), who reported a substantial reduction in grazing land.

The decline in the bare land was attributed to the widespread implementation of plantations (afforestation and reforestation), soil and water conservation activities, and area closure efforts. Similar results were observed in the Upper Baro basin and Bilate watershed (Shibeshi & Venkatesham, 2024; Engida *et al*., 2021). However, this result contradicts the findings of Mariye *et al*. (2023) and Ogato *et al*. (2021), who stated that bare land area increased due to the overutilization of cultivated land, grassland, and shrub/bushland. Previous results from various parts of Ethiopia indicated a consistent expansion of agricultural land and urban built-up areas (Bihon *et al*., 2025; Dibaba *et al*., 2020; Miheretu & Yimer, 2017), whereas grazing and bare land areas steadily declined.

The projections were conducted for the years 2034 and 2044 using the CA-Markov model. The overall accuracy assessment result indicates a moderate level of agreement between the two map categories. The simulation results indicate that cropland, water bodies, forest land, and built-up areas are likely to continue increasing in 2034 and 2044. This is an apparent indicator of a continued human disturbance in the study landscape. The increase in settlement and cropland would be attributable to rising demand for infrastructure development and crop production to support the fast-growing population. In line with this, a study by Molla *et al*. (2024) indicates that the built-up areas of Hawassa city are projected to increase by approximately 1,070.82 hectares between 2021 and 2050. Additionally, national policies, such as the agricultural development-led industrialization strategy, have influenced land use patterns (Molla *et al*., 2024). These policies have promoted agricultural intensification, resulting in both the expansion of cultivated areas and increased competition for land.

The expansion of crop land into forest land, grazing, and bare land has reduced the availability of essential ecosystem services such as fuelwood, fodder, water balance, and soil fertility (Wubie *et al*., 2016) and could intensify households' exposure to environmental risks such as droughts and floods by removing natural buffers and safety nets. For instance, the loss of grazing land due to agricultural expansion has weakened the resilience of livestock-dependent communities, resulting in declining income and food insecurity (Tofu *et al*., 2023). Urban expansion into fertile agricultural lands can displace smallholder farmers, particularly around major towns and cities (Ayenachew & Abebe, 2024). Collectively, these changes illustrate how shifts in land use, if not managed sustainably, can increase livelihood vulnerability, especially for those already at risk due to poverty and climatic variability.

CONCLUSION

This study provides valuable insights into the dynamics of land transformation over the past two decades and future projections of changes using advanced methodologies, including the RF and CA-ANN machine learning algorithms for LULC classification and future projection, respectively. The result demonstrates a consistent increase in cropland, water bodies, and built-up areas over the study period. In contrast, grazing land and bare land have declined, indicating a significant land use land cover transition driven by agricultural intensification and urban expansion. Notably, forest land has increased steadily, underscoring the potential for reforestation and afforestation efforts. The predicted figures for 2034 and 2044 show continued growth in cropland, water bodies, and forest land; however, the rate of increase slightly declines after 2034. Built-up areas are expected to increase significantly, especially in the urban center, with a predicted increase of 10328.15 ha between 2034 and 2044. In contrast, grazing land and bare land are expected to experience a further decline. In general, the Jemma sub-basin is undergoing significant land use and land cover changes that will shape its future ecological and socioeconomic landscape. Therefore, implementing sustainable land management practices, community-based conservation efforts, and comprehensive urban planning will be pivotal in maintaining the delicate balance between development and environmental conservation. This study used remotely sensed data, GEE, RF, and CA-ANN algorithms to analyse the past and future LULCC of the Jemma sub-basin. In addition, we used different vegetation indices to improve the classification accuracy. This integrated methodology provided a reproducible framework for monitoring environmental changes and a scientifically rigorous approach to future spatiotemporal LULCC assessments, applicable across different regions and time periods. Future studies, such as the real cause/ factor for forest increase, both socio-economic and ecological drivers of land use land cover change in the Jemma sub-basin, are recommended to better understand the implications for local livelihoods and regional development.

ACKNOWLEDGMENTS

The authors would like to thank the FG and KI respondents for their kind responses.

CONFLICTS OF INTEREST

The authors declare no conflict of interest.

REFERENCES

ABDO (2020). *Wter Atlas of Abbay Basin*.

Abebe, G., Getachew, D., & Ewunetu, A. (2021). Analysing land use / land cover changes and its dynamics using remote sensing and GIS in Gubalafito district , Northeastern Ethiopia. *SN Applied Sciences*, *December*. https://doi.org/10.1007/s42452-021-04915-8

Agona, Y., & Abebe, B.G. (2024). The dynamics of urbanization , land use land cover changes , and land expropriation in Addis Ababa ,. *Frontiers in Environmental Science*, *August*, 1–11. https://doi.org/10.3389/fenvs.2024.1439954

Al, A., Huda, N., Subramanyam, G., Faisal, A.-, Uddin, N., Al, A., & Akter, M. (2021). Cellular Automata approach in dynamic modelling of land cover changes using RapidEye images in Dhaka, Bangladesh. *Environmental Challenges*, *4*, 100084. https://doi.org/10.1016/j.envc.2021.100084

Alawamy, J.S., Balasundram, S.K., Husni, A., Hanif, M., Teh, C., & Sung, B. (2020). Detecting and Analyzing Land Use and Land Cover Changes in the Region of Al - Jabal Al -

Akhdar , Libya Using Time - series Landsat Data from 1985 to 2017. *Sustainability (Switzerland)*. https://doi.org/10.3390/su12114490

Albut, S. (2024). *Land Use Change Utilizing the QGIS MOLUSCE Plugin*. *December 2024*.

Ali, Y.S.A., Crosato, A., & Mohamed, Y.A. (2015). Sediment balances in the Blue Nile River Basin. *International Journal of Sediment Research*, *29*(3), 316–328. https://doi.org/10.1016/S1001-6279(14)60047-0

Amani, M., Limited, I.C., Ghorbanian, A., Ahmadi, S.A., & Kakooei, M. (2020). Google Earth Engine Cloud Computing Platform for Remote Sensing Big Data Applications : A Comprehensive Review. *Journal of selected topics in applied earth observations and remote sensing*, *September*. https://doi.org/10.1109/JSTARS.2020.3021052

Amani, M., Mahdavi, S., Afshar, M., Brisco, B., Huang, W., Mohammad, S., Mirzadeh, J., White, L., Banks, S., Montgomery, J., & Hopkinson, C. (2019). Canadian Wetland Inventory using Google Earth Engine : The First Map and Preliminary Results. *Remote Sensing*, 1–20. https://doi.org/10.3390/rs11070842

Amiga, A., Tolossa, D., & Damte, A. (2024). Land Use Policy Eucalyptus tree expansion and land use and land cover dynamics in Ethiopia- empirical evidence from Gurage Zone , Ethiopia. *Land Use Policy*, *141*(March), 107149. https://doi.org/10.1016/j.landusepol. 2024.107149

Ayenachew, Y.A., & Abebe, B.G. (2024). Navigating urbanization implications : effects of land expropriation on farmers ' livelihoods in Addis Ababa , Ethiopia. *Frontiers in Sustainable Cities*, *June*, 1–13. https://doi.org/10.3389/frsc.2024.1385309

Baig, M.F., Petronas, U.T., Raza, M., Mustafa, U., Petronas, U.T., & Baig, I. (2022). Assessment of Land Use Land Cover Changes and Future Predictions Using CA-ANN Simulation for Selangor, Malaysia. *Water*, *February*. https://doi.org/10.3390/w14030402

Beijma, S. Van, Comber, A., & Lamb, A. (2014). Random forest classi fi cation of salt marsh vegetation habitats using quad-polarimetric airborne SAR , elevation and optical RS data. *Remote Sensing of Environment*, *149*, 118–129. https://doi.org/10.1016/j.rse.2014.04.010

Belay, F., Mulugeta, M., & Makonnen, T. (2023). Land use land cover change and expansion of Eucalyptus plantations in Senan District, northwest Ethiopia: analysis of potential factors. *Ethiopian Journal of Environment and Development*, *5*(2), 23–36. https://doi.org/10.20372/ejed.v05i2.03

Betrie, G.D., Mohamed, Y.A., Van Griensven, A., & Srinivasan, R. (2011). Sediment management modelling in the Blue Nile Basin using SWAT model. *Hydrology and Earth System Sciences*, *15*(3), 807–818. https://doi.org/10.5194/hess-15-807-2011

Betru, T., Tolera, M., Sahle, K., & Kassa, H. (2019). Trends and drivers of land use/land cover change in Western Ethiopia. *Applied Geography*, *104*(February), 83–93. https://doi.org/10.1016/j.apgeog.2019.02.007

Bihon, Y.T., Mohammed, A.K., & Ayele, E.G. (2025). Spatiotemporal analysis of land use and land cover using random forest in Google Earth engine : A case study of the Grand Ethiopian Renaissance Dam basin and reservoir , Upper Blue Nile , Ethiopia. *Environmental Challenges*, *21*(August), 101311. https://doi.org/10.1016/j.envc.2025.101311

Braun, E.N.A.M.J. von. (2016). Economics of Land Degradation and Improvement – A Global Degradation and Sustainable Development. In *Springer*. https://doi.org/10.1007/ 978-3-319-19168-3_3

Cherinet, A. (2019). Climate Change/Variability Impacts on Farmers livelihoods and Adaptation Strategies: In the Case of Ensaro District, Ethiopia. *International Journal of*

Environmental Sciences & Natural Resources, *18*(1), 1–7. https://doi.org/10.19080/ijesnr.2019.18.555976

CSA. (2007). *Population and Housing Census 2007 Report*. http://www.csa.gov.et/surveys/Population and Housing census/ETH-pop-2007/survey0/data/Doc/Reports/National_Statistical.pdf

Dagnachew, M.E.D., Ebede, A.S.K., Oges, A.W.M., & Bebe, A.D.A. (2020). Land Use Land Cover Changes and Its drivers in Gojeb River Catchment , Omo Gibe Basin , Ethiopia. *Journal of Agriculture and Environment for International Development*, *114*(1), 33–56. https://doi.org/10.12895/jaeid.20201.842

Dibaba, W., Demissie, T.A., & Konrad, M. (2020). Drivers and Implications of Land Use/Land Cover Dynamics in Finchaa Catchment, Northwestern Ethiopia. *Land*, 1–20.

EFD. (2024). *National Forest Cover Mapping Report for the year 2023*. *April*.

Engida, T.G., Nigussie, T.A., Aneseyee, A.B., & Barnabas, J. (2021). Land Use / Land Cover Change Impact on Hydrological Process in the Upper Baro Basin , Ethiopia. *Hindawi*, *July*.

Eshetie, A.A., Wubneh, M.A., Kifelew, M.S., & Alemu, M.G. (2023). Application of artificial neural network (ANN) for investigation of the impact of past and future land use – land cover change on streamflow in the Upper Gilgel Abay watershed , Abay Basin ,. *Applied Water Science*, *13*(11), 1–22. https://doi.org/10.1007/s13201-023-02003-3

Feyissa, G., & Gebremariam, E. (2018). Mapping of Landscape Structure and Forest Cover Change Detection in the Mountain Chains around Addis Ababa: The Case of Wechecha Mountain, Ethiopia. *Remote Sensing Applications: Society and Environment*. https://doi.org/10.1016/j.rsase.2018.07.008

Gashaw, T., Tulu, T., Argaw, M., & Worqlul, A.W. (2017). Evaluation and prediction of land use/land cover changes in the Andassa watershed, Blue Nile Basin, Ethiopia. *Environmental Systems Research*, *6*(1). https://doi.org/10.1186/s40068-017-0094-5

Gasirabo, A., Xi, C., Hamad, B.R., & Edovia, U.D. (2023). A CA – Markov-Based Simulation and Prediction of LULC Changes over the Nyabarongo River Basin , Rwanda. *Land*.

Gebrehiwot, S.G., Bewket, W., Gärdenäs, A.I., & Bishop, K. (2014). Forest cover change over four decades in the Blue Nile Basin, Ethiopia: Comparison of three watersheds. *Regional Environmental Change*, *14*(1), 253–266. https://doi.org/10.1007/s10113-013-0483-x

Gorelick, N., Hancher, M., Dixon, M., Ilyushchenko, S., Thau, D., & Moore, R. (2017). Remote Sensing of Environment Google Earth Engine : Planetary-scale geospatial analysis for everyone. *Remote Sensing of Environment*, *202*, 18–27. https://doi.org/10.1016/j.rse.2017.06.031

Hailu, A., Mammo, S., & Kidane, M. (2020). Land Use Policy Dynamics of land use , land cover change trend and its drivers in Jimma Geneti District , Western Ethiopia. *Land Use Policy*, *99*(August), 105011. https://doi.org/10.1016/j.landusepol.2020.105011

Halefom, A., Teshome, A., Sisay, E., & Ahmad, I. (2018). Dynamics of Land Use and Land Cover Change Using Remote Sensing and GIS : A Case Study of. *Journal of Geographic Information System*, 165–174. https://doi.org/10.4236/jgis.2018.102008

He, X., & Chen, Z. (2022). Weather , cropland expansion , and deforestation in Ethiopia. *JOurnal of Environmental Economica and Management*, *111*(November 2021). https://doi.org/10.1016/j.jeem.2021.102586

Hishe, H., Giday, K., Orshoven, J. Van, Muys, B., Taheri, F., Azadi, H., Feng, L., Zamani, O., Mirzaei, M., & Witlox, F. (2020). Land Use Policy Analysis of Land Use Land Cover Dynamics and Driving Factors in Desa ' a Forest in Northern Ethiopia. *Land Use Policy*, *January*, 105039. https://doi.org/10.1016/j.landusepol.2020.105039

Kafy, A., Dey, N.N., Rakib, A. Al, Rahaman, Z.A., Nasher, N.M.R., & Bhatt, A. (2021). Modeling the relationship between land use / land cover and land surface temperature in Dhaka , Bangladesh using CA-ANN algorithm. *Environmental Challenges*, *4*(July), 100190. https://doi.org/10.1016/j.envc.2021.100190

Kasahun, M., & Legesse, A. (2024). Machine learning for urban land use / cover mapping : Comparison of artificial neural network , random forest and support vector machine , a case study of Dilla town. *Heliyon*, *10*(20), e39146. https://doi.org/10.1016/j.heliyon.2024.e39146

Kuma, H.G., Feyessa, F.F., & Demissie, T.A. (2022). Land-use / land-cover changes and implications in Southern Ethiopia : evidence from remote sensing and informants. *Heliyon*, *8*(December 2021), e09071. https://doi.org/10.1016/j.heliyon.2022.e09071

Leta, M.K., & Demissie, T.A. (2021). Modeling and Prediction of Land Use Land Cover Change Dynamics Based on Land Change Modeler (LCM) in Nashe Watershed , Upper Blue Nile Basin , Ethiopia. *Sustainability (Switzerland)*, *Lcm*.

Li, J., Wang, Z., Wu, X., Zscheischler, J., Guo, S., & Chen, X. (2021). *A standardized index for assessing sub-monthly compound dry and hot conditions with application in China*. 1587–1601.

Lisa C. Kelley, L.P. and C.B. (2018). Using Google Earth Engine to Map Complex Shade-Grown Coffee Landscapes in Northern Nicaragua. *Remote Sensing*. https://doi.org/10.3390/rs10060952

Mahdianpari, M., Salehi, B., Mohammadimanesh, F., & Motagh, M. (2017). Random forest wetland classification using ALOS-2 L-band , RADARSAT-2 C-band , and TerraSAR-X imagery. *ISPRS Journal of Photogrammetry and Remote Sensing*, *130*, 13–31. https://doi.org/10.1016/j.isprsjprs.2017.05.010

Mare, Y., Bitew, D., & Zewotir, T. (2024). Linear modeling of zonal level crop production in Ethiopia. *Heliyon*, *10*(10), e30951. https://doi.org/10.1016/j.heliyon.2024.e30951

Mariye, M., Jianhua, L., & Maryo, M. (2023). Land use land cover change analysis and detection of its drivers using geospatial techniques : a case of south-central Ethiopia. *All Earth*, *34*(1), 309–332. https://doi.org/10.1080/27669645.2022.2139023

Mekuria, W., Mekonnen, K., Thorne, P., Bezabih, M., & Tamene, L. (2018). Competition for land resources : driving forces and consequences in crop-livestock production systems of the Ethiopian highlands. *Ecological Processes*.

Millard, K., & Richardson, M. (2015). On the Importance of Training Data Sample Selection in Random Forest Image Classification: A Case Study in Peatland Ecosystem Mapping. *Remote Sensing*, 8489–8515. https://doi.org/10.3390/rs70708489

Minta, M., Kibret, K., Thorne, P., Nigussie, T., & Nigatu, L. (2018). Land use and land cover dynamics in Dendi-Jeldu hilly-mountainous areas in the central Ethiopian highlands. *Geoderma*, *314*(May 2017), 27–36. https://doi.org/10.1016/j.geoderma.2017.10.035

Moisa, M.B., Dejene, I.N., Roba, Z.R., & Gemeda, D.O. (2022). Impact of urban land use and land cover change on urban heat island and urban thermal comfort level : a case study of Addis Ababa City , Ethiopia. *Environmental Monitoring and Assessment*, *September*. https://doi.org/10.1007/s10661-022-10414-z

Molla, G., & Addisie, M.B. (2023). Expansion of Eucalyptus Plantation on Fertile Cultivated

Lands in the North-Western Highlands of Ethiopia. *Remote Sensing*, 1–16.

Molla, M.B., Gelebo, G., & Girma, G. (2024). Urban expansion and agricultural land loss : a GIS-Based analysis and policy implications in Hawassa city , Ethiopia. *Fontiers in Environmental Science*, *November*. https://doi.org/10.3389/fenvs.2024.1499804

Negasa, D.J., Environment, E., Mbilinyi, B.P., & Mahoo, F. (2016). Evaluation of Land Use / Land Cover Changes and Eucalyptus Expansion in Meja Watershed , Ethiopia. *Journal of Geography, Environment and Earth Science International*, *January*. https://doi.org/10.9734/JGEESI/2016/26606

Ogato, G.S., Bantider, A., & Geneletti, D. (2021). Dynamics of land use and land cover changes in Huluka watershed of Oromia Regional State , Ethiopia. *Environmental Systems Research*. https://doi.org/10.1186/s40068-021-00218-4

Oloukoi, J. (2018). *Rate Of Land Cover Change And Its Determinants In The Soudano-Guinea Transition Zone Of Benin Republic*. *June*. https://doi.org/10.4314/ejesm.v10i5.12

Pande, C.B., Srivastava, A., Moharir, K.N., Radwan, N., & Sidek, L.M. (2024). Characterizing land use / land cover change dynamics by an enhanced random forest machine learning model : a Google Earth Engine implementation. *Environmental Sciences Europe*. https://doi.org/10.1186/s12302-024-00901-0

Regasa, M.S., Nones, M., & Adeba, D. (2021). A Review on Land Use and Land Cover Change in Ethiopian Basins A Review on Land Use and Land Cover Change in Ethiopian Basins. *Land*, *June*. https://doi.org/10.3390/land10060585

Rehman, A., Qin, J., Pervez, A., Khan, M.S., Ullah, S., & Ahmad, K. (2022). *Land-Use / Land Cover Changes Contribute to Land Surface Temperature : A Land-Use / Land Cover Changes Contribute to Land Surface Temperature : A Case Study of the Upper Indus Basin of Pakistan*. *January*. https://doi.org/10.3390/su14020934

Sarkar, A. (2019). Accuracy Assessment and Analysis of Land Use Land Cover Change Using Geoinformatics Technique in Raniganj Coalfield Area , India. *International Journal of Research and Analytical Reviews*, *February 2019*.

Shibeshi, S., & Venkatesham, B. (2024). Land use land cover change as a casual factor for climate variability and trends in the Bilate Watershed , Ethiopia. *Environmental Monitoring and Assessment*, *196*(12), 1–19. https://doi.org/10.1007/s10661-024-13435-y

Shixu Wang, Zulu Zhang, X. W. (2014). Land use change and prediction in the Baimahe Basin using GIS and CA-Markov model L-. *International Symposium on Remot Sensing of Environment*. https://doi.org/10.1088/1755-1315/17/1/012074

Sousa, C. De, Lola, F., Neigh, C., & Boucka, F. (2020). Cloud-computing and machine learning in support of country-level land cover and ecosystem extent mapping in Liberia and. *PLoS ONE*, 1–24.

Tadese, S., Soromessa, T., & Bekele, T. (2021). Analysis of the Current and Future Prediction of Land Use / Land Cover Change Using Remote Sensing and the CA-Markov Model in Majang Forest Biosphere Reserves of Gambella , Southwestern Ethiopia. *Hindawi*. https://doi.org/10.1155/2021/6685045

Temeche, D., Getachew, E., & Hailu, G. (2021). Effects of Nitrogen Fertilizer Quantity and Time of Application on Sorghum (Sorghum bicolor (L .) Moench) Production in Lowland Areas of North Shewa , Ethiopia. *Hindawi*, *2021*, 1–8. https://doi.org/10.1155/2021/3019528

Tessema, N., Kebede, A., & Yadeta, D. (2020). Modeling land use dynamics in the Kesem sub- basin , Awash River basin , Ethiopia. *Cogent Environmental Science*, *6*(1). https://doi.org/10.1080/23311843.2020.1782006

Tewabe, D., & Fentahun, T. (2020). Assessing land use and land cover change detection using remote sensing in the Lake Tana Basin , Northwest Ethiopia Assessing land use and land cover change detection using remote sensing in the Lake Tana Basin , Northwest Ethiopia. *Cogent Environmental Science*, *6*(1). https://doi.org/10.1080/23311843.2020.1778998

Tofu, D.A., Fana, C., Dilbato, T., Dirbaba, N.B., & Tesso, G. (2023). Pastoralists ' and agro - pastoralists ' livelihood resilience to climate change - induced risks in the Borana zone , south Ethiopia : Using resilience index measurement approach. *Pastoralism*. https://doi.org/10.1186/s13570-022-00263-3

Tolentino, F.M., Lourdes, M. De, & Trindade, B. (2021). Selecting features for LULC simultaneous classification of ambiguous classes by artificial neural network. *Remote Sensing Applications: Society and Environment*, *24* (August), 100616. https://doi.org/10.1016/j.rsase.2021.100616

Tolessa, T., Senbeta, F., & Kidane, M. (2017). The impact of land use/land cover change on ecosystem services in the central highlands of Ethiopia. *Ecosystem Services*, *23*(June 2016), 47–54. https://doi.org/10.1016/j.ecoser.2016.11.010

Wasie, A. (2024). Determinant Factors of " Eucalyptus globulus " (Labill .) Woodlot Production in Tach Gayint District , South Gondar Zone , Amhara Region , Ethiopia. *International Journal of Forestry Research*, *2024*. https://doi.org/10.1155/2024/1460164

Worku, G., Teferi, E., Bantider, A., & Dile, Y. T. (2021). Climate Risk Management Modelling hydrological processes under climate change scenarios in the Jemma sub-basin of upper Blue Nile Basin , Ethiopia. *Climate Risk Management*, *31*(January), 100272. https://doi.org/10.1016/j.crm.2021.100272

Wubie, M. A., Assen, M., & Nicolau, M. D. (2016). Patterns , causes and consequences of land use / cover dynamics in the Gumara watershed of lake Tana basin , Northwestern Ethiopia. *Environmental Systems Research*, 1–12. https://doi.org/10.1186/s40068-016-0058-1

Xie, Z., Chen, Y., Lu, D., & Li, G. (2019). Classification of Land Cover , Forest , and Tree Species Classes with ZiYuan-3 Multispectral and Stereo Data. *Remote Sensing*, 1–27. https://doi.org/10.3390/rs11020164

Zhao, Z., Islam, F., Waseem, L.A., Tariq, A., Nawaz, M., Islam, I.U., Bibi, T., Rehman, N. U., Ahmad, W., Aslam, R. W., Raza, D., & Hatamleh, W. A. (2023). Comparison of Three Machine Learning Algorithms Using Google Earth Engine for Land Use Land Cover Classification. *Rangeland Ecology & Management*, *92*(November), 129–137. https://doi.org/10.1016/j.rama.2023.10.007